David Tomás Sánchez Martínez
Lourdes García Rodríguez
(coordinadores)

Proceedings of the 7th International Seminar on ORC Power Systems

Editorial Universidad de Sevilla

Proceedings of the 7th International Seminar on

ORC
Power Systems

David Tomás Sánchez Martínez
Lourdes García Rodríguez
(coordinadores)

Proceedings of the 7th International Seminar on

ORC Power Systems

(ORC2023)

4th to 6th
SEPTEMBER
SEVILLE 2023

EDITORIAL UNIVERSIDAD DE SEVILLA

Sevilla, 2024

Colección Actas
Núm.: 91

Review chairs of the 7th Internation Seminar on ORC Power Systems

Prof. Christoph Wieland (University of Duisburg-Essen) - *Review Chair*
Prof. Sotirios Karellas (National Technical University of Athens) - *Review Co-Chair*
Prof. Teemu Turunen-Saaresti (LUT University) - *Review Co-Chair*
Dr. Diego-César Alarcón-Padilla (Plataforma Solar de Almería - CIEMAT) - *Review Co-Chair*
Dr. Francesco Crespi (Universidad de Sevilla) - *Review Co-Chair*

c/ Porvenir, 27 - 41013 Sevilla.
Tlfs.: 954 487 447; 954 487 451; Fax: 954 487 443
Correo electrónico: info-eus@us.es
Web: https://editorial.us.es

ISBN 978-84-472-2745-7
DOI: https://dx.doi.org/10.12795/9788447227457

Diseño de cubierta y maquetación: los autores

INDEX OF CONTRIBUTIONS

DOI: https://dx.doi.org/10.12795/9788447227457_97

Basic design of an ORC demonstrator system for implementation in an Iron & Steel plant through the DECAGONE project

Magnus Windfeldt[1], Han Deng[1], Trond Andresen[1,*], Christopher Schifflechner[2]

[1] *SINTEF Energy Research, Trondheim, Norway*
[2] *Technical University of Munich, Munich, Germany*

*Corresponding Author: trond.andresen@sintef.no

ABSTRACT

Waste heat recovery (WHR) technologies offer great opportunities for improving energy efficiency and reducing CO_2 emissions for energy intensive industrial processes. The DECAGONE project is developing an innovative ORC-based WHR system to be demonstrated in an iron & steel plant located in the Czech Republic. The design of the ORC system considers the practical site-specific conditions and limitations, such as variations in heat source conditions, heat sink availability, and size and space limitations for the ORC components. Various cycle configurations are compared with a thermodynamic optimization model for maximizing the net power output subject to the process constraints, including (1) recuperative vs. non-recuperative designs, (2) air vs. water as heat sink and (3) direct vs. indirect evaporation. The recuperative cycle with indirect evaporation and direct air condensation is deemed the most suitable solution for the project site conditions. The results provide recommendations for performance improvement and indications for performance subject to practical plant operating conditions, such as large range of temperature and flow rate of waste heat source. Analyses in this work provide the basis for detailed component design and decision processes towards finalizing the design of the demonstrator. 574

1 INTRODUCTION

As energy availability decreases and incentives for reducing energy consumption and greenhouse gas emissions increases, energy efficiency measures become increasingly interesting for energy intensive industries. IEA reports (IEA, 2021) that rapid implementation of waste heat recovery solutions in this sector is critical for reaching net zero emissions by 2050, and a recovery potential approaching 300 TWh/year from industrial thermal processes in the EU has been estimated (Bianchi *et al.*, 2019).

The DECAGONE project (Demonstrator of industrial carbon-free power generation from ORC-based waste-heat-to-energy-systems, https://decagone.eu/), funded by Horizon Europe, is developing an innovative ORC-based WHR system to be constructed, integrated, and demonstrated in Třinec Iron and Steel Works in the Czech Republic. Outcomes of the demonstration will be evaluated in terms of potential market and transposability at the European scale for other significant industrial sectors. The overarching goals of this project is to make ORC systems more efficient, more cost-effective, and more adaptable to various industrial sectors in order to increase their rate of implementation.

In the current work, a basic optimization of operating conditions is performed of the entire system comprising the ORC cycle and heat recovery loop, based on measured conditions and practical limitations at the demonstration site. This will provide the first realistic estimate of system performance at the chosen nominal operation point, and will serve as the basis for performance specification and design of all main system components. Thus, some design choices have been made prior to the present work, such as working fluid and cycle layout, while some assumptions are made regarding component performance that will be subject of further study in following work. In addition to the chosen cycle layout, other design options are explored for their impact on system performance and requirements. This includes solutions deemed unfeasible at the demonstration site, but that could be interesting in other industrial applications.

2 METHODOLOGY

2.1 Problem description

The goal of this work is to compare the performance impact of design choices and alternatives for an ORC recovering waste heat from an iron & steel plant, and for each alternative identify optimized operating conditions while satisfying specific and practical plant conditions. Historic site data from 1.5 years of operation have shown that the flue gas temperature ranges from 400 °C to 500 °C and the volume flow rate ranges from 40 000 Nm^3/h to 80 000 Nm^3/h. Values of 465 °C and 71 000 Nm^3/h are chosen as the design point based on a preceding data analysis, which identified these as the most representative operating conditions.

Collected site data covering one year shows that the ambient temperature ranges from −5 °C in winter to 30 °C in summer. A nominal value of 12.5 °C is chosen for the design point, to be used as the heat sink temperature and as a reference for exergy calculations. Apart from the heat source and sink, the ORC systems will be optimized for maximum power output against other practical constraints, which will be detailed later.

2.2 ORC layout basis

The ORC configuration used as basis for the system modelling and comparison of various design options is illustrated in Figure 1. This configuration includes four fluid circuits: The heat source stream, the indirect fluid loop, the working fluid loop, and the heat sink stream. Therminol66, a commercially available thermal oil, is used as the indirect fluid to extract the heat from the source via the waste heat recovery heat exchanger (WHR HX), and supply the heat for the working fluid loop via the evaporator. Additionally, a bypass of the heated indirect fluid will go to the thermal energy storage (TES) to store the energy when the recovered heat from WHR HX exceeds the heat supplied to the working fluid loop. Cyclopentane is selected as the working fluid which is heated in the evaporator and expand in the turbine to generate power. While the choice of working fluid is beyond the scope of the present work, the use of cyclopentane is justified in the larger project context based on its high suitability for high-temperature ORC applications (Lai *et al*,. 2011), both as a pure fluid and in a zeotropic mixture (Braimakis *et al*., 2015). It has an Ozone Depletion Potential of zero and a Global Warming Potential below 25 (EPA, 2013), and is already commercially applied in existing ORC systems (Lecompte *et al*., 2015). 575

The layout in Figure 1 is a recuperative design, in which a recuperator is used to recover the heat from the hot turbine outlet and heat up the cold working fluid after it is cooled in the condenser and pumped. The pressure drop for the heat source and heat sink inside the heat exchangers is compensated with the flue gas pump and air fan, so that the pressure of heat source and heat sink out from the system is the same as that into the system.

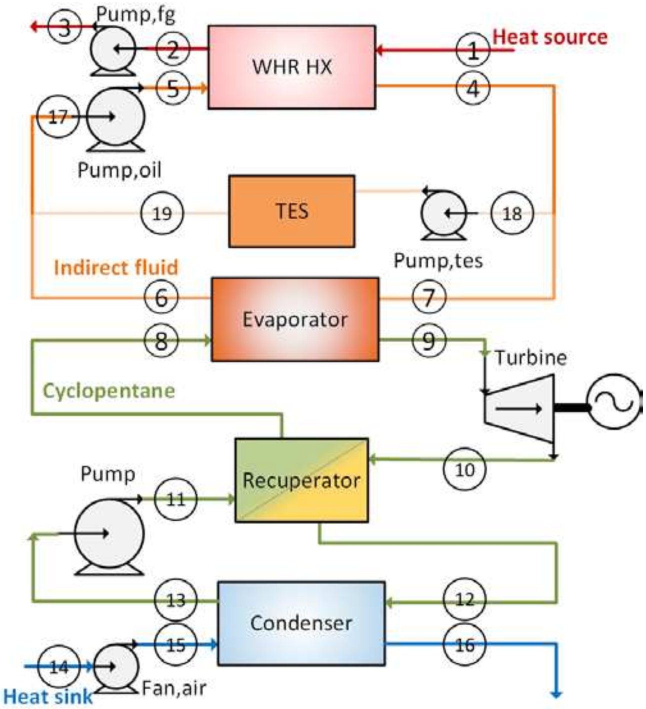

Figure 1: ORC layout for modelling the base case

2.3 System optimization model

The system optimization model combines a steady-state thermodynamic model simulating the system and component performance with an optimization algorithm to find the optimum solution for the given objective function. The model is developed using an in-house framework described in detail in previous work (Deng *et al.* 2020, Hagen *et al.* 2020, Deng *et al.* 2022). The steady-state thermodynamic model is built based on the layout shown in Figure 1, but is flexible to be adapted to other configurations. For example, a non-recuperative cycle can be represented by simply redefining state points 10 and 12 to be equal, and similarly for state points 11 and 13. 576

The steady-state thermodynamic model is built by connecting different sub-models specific for each component. The turbine is modelled based on an isentropic expansion process corrected by an isentropic efficiency, and the power generated is further corrected by a mechanical efficiency. Similarly, an isentropic or isochoric compression process with the efficiency correction is used for the calculation of the pumps and fans, and the power consumption is corrected by a mechanical efficiency. Constant values are used for all efficiencies, which assumes that for each resulting set of operating conditions in explored cases, the relevant components can be individually designed to reach or surpass the defined efficiency. This work does not consider off-design performance.

The heat exchangers are calculated based on the heat balance between the cold and hot side, assuming a counter-current flow. The local temperature differences across each heat exchanger is found by discretizing the heat exchanger into the certain number of sections with equal heat duty and pressure drop, and the UA value of the heat exchanger is then also found as the sum of the local UA values calculated for each section. Sufficient discretization of the heat exchanger can ensure accurate temperature profiles and UA values also for heat exchangers where phase change of a fluid occurs.

For simplicity, the inlet and outlet conditions of the indirect fluid on the thermal energy storage bypass (points 18 and 19) are assumed to be the same as in and out of the evaporator (points 7 and 6). The mass flow rate for the bypass is calculated from a specified TES duty and the enthalpy difference between the inlet and outlet. Then, the mass flow rate of the indirect fluid in the WHR HX is the sum of its mass flow rate through the TES and the evaporator.

For the thermodynamic properties, the flue gas, the working fluid cyclopentane, and the heat sink are calculated using the REFPROP 9.1 library (Bell 2013). The properties of Therminol66 are fitted to the distributor's data sheet and validated using the open-source library CoolProp (Bell *et al.* 2014).

The optimization problem is solved by the gradient-based constrained optimization solver NLPQL (Schittkowski 1986) in a framework which allows for flexibility in the definition of variables, constraints, and objection function. The net power W_{net} is to be maximized as

$$W_{net} = W_{turbine} - W_{fan,fg} - W_{pump,oil} - W_{pump,wf} - W_{fan,air} \quad (1)$$

with W_i being the electrical power produced or consumed by the indicated component. The variables and constraints are set as shown in Table 1, together with other fixed parameters. Some practical limitations are set as the boundary of the variables instead of constraints, such as the minimum allowable flue gas outlet temperature being constrained by the lower limit of the variable. Please note that the specified variable range does not represent the variation in resulting values, it is simply the allowed range provided to the solver. For given values of input variables, the system and components performance are calculated with the models described in the above section. Then the partial derivatives of the objective and constraint functions to the variables are estimated, and the gradient information is used by the NLPQL solver to propose new values for the free variables for the next iteration. The problem is solved when the maximum value of the objective function is found and all the constraints are satisfied.

Table 1: Optimization setup: Variables, constraints, and fixed parameters with their set input values or allowable min-max ranges.

Variables	**State point (symbols)**	**Range/Value**
Flue gas outlet temperature	T_2	150 – 300 °C
Indirect fluid evaporator outlet temperature	T_6	50 – 200 °C
Indirect fluid evaporator temperature change	ΔT_{7-6}	110 – 250 K
Turbine inlet pressure	P_9	15 – 38 bar
Turbine inlet temperature	T_9	50 – 275 °C
Working fluid condenser outlet pressure	P_{13}	0.3 – 2.5 bar
Heat sink temperature increase	ΔT_{16-15}	10 – 15 K
Recuperator effectiveness	$\eta_{recup}: (h_{10} - h_{12})/(h_{10} - h_{11})$	0.05 – 0.95
Constraints		
Min. pinch point temperature difference	$\Delta T_{\min,WHRHX}/\Delta T_{\min,recup}$	40 / 20 K
Min. temperature difference at bubble point	$\Delta T_{\min,evap}$	20 K
Min. temperature difference at the cold end	$\Delta T_{\min,cond}$	24 K
Max. indirect fluid temperature	$T_{\max,4}$	310 °C
Max. working fluid pressure	$P_{\max,11}$	38 bar
Fixed parameters		
Isentropic efficiencies	$\eta_{pump,fg}/\eta_{pump,wf}/\eta_{turbine}$	0.7 / 0.7 / 0.8
Isochoric efficiencies	$\eta_{fan,air}/\eta_{pump,oil}$	0.63 / 0.7
Motor/generator efficiencies	$\mathrm{H}_{pump,fg}/\mathrm{H}_{pump,wf}/\mathrm{H}_{turbine}$ / $\mathrm{H}_{fan,air}/\mathrm{H}_{pump,oil}$	0.9 / 0.9 / 0.97/ 0.9 / 0.9
Pressure drop of the cold sides in the HXs	$\Delta P_{WHRHX}/\Delta P_{evap}/$ $\Delta P_{recup}/\Delta P_{cond}$	100 / 100 / 50 / 0.15 kPa
Pressure drop of the hot sides in the HXs	$\Delta P_{WHRHX}/\Delta P_{evap}/$ $\Delta P_{recup}/\Delta P_{cond}$	0.5 / 100 / 6 / 12 kPa

2.4 Alternative cycle layouts

Apart from the base case layout shown in Figure 1, other common design options with layouts as shown in Figure 2, have been optimized under the same conditions in order to quantify the impact of design alternatives.

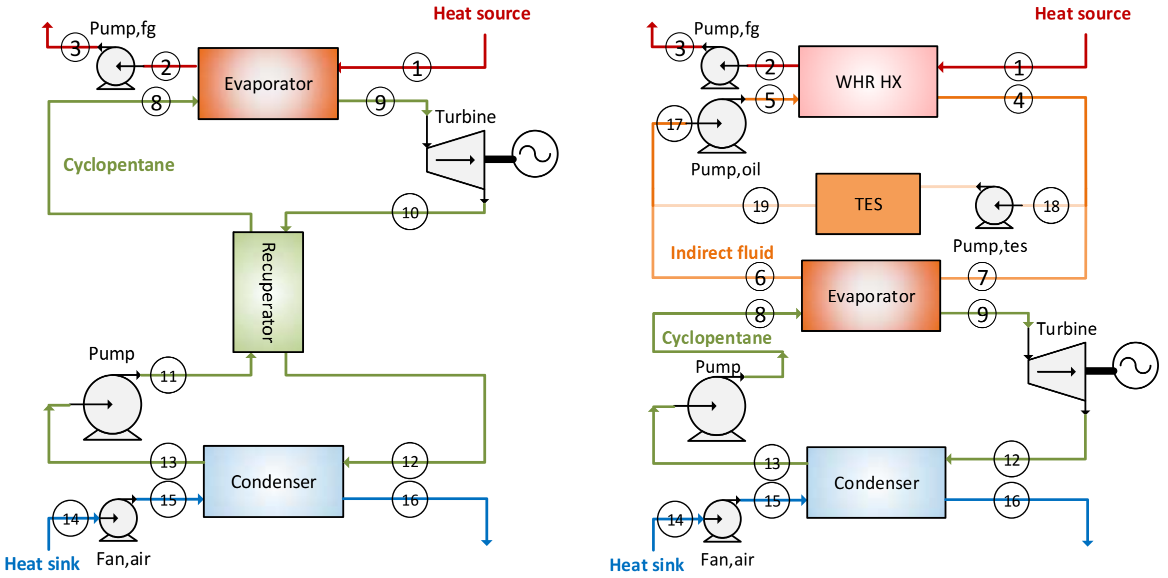

(a) Direct evaporation design (b) Non-recuperative design

Figure 2: Other ORC configurations with (a) direct evaporation (b) non-recuperative design

The direct evaporation design in Figure 2(a) removes the indirect fluid circuit and the thermal energy storage. It enables recovering heat from the flue gas in slightly larger quantities or at higher 578 temperatures, and saves both space and costs of components in the indirect fluid circuit. However, direct heat recovery using the flammable cyclopentane in this application is considered unfeasible for several reasons, such as direct exposure to high temperatures, high fluid charge in contact with the flue gas flow, and poor provisions for buffering of the variable heat source energy. The direct evaporation case is still included to indicate the overall performance difference compared to the chosen indirect system. The non-recuperative design in Figure 2(b), compared with the recuperative design in Figure 1, saves cost, space and pressure drop for the recuperator and pipelines. However, it shifts more cooling duty to the condenser and heating duty to the evaporator which will require these to be larger. The optimization of the non-recuperative design uses the same settings as the recuperative design, where the recuperator is deactivated by setting both the recuperative efficiency and fluid pressure drops to value of 0.

The condenser is expected to be the largest component in the ORC system if using direct air cooling. As the available site space is limited, three additional condensation options are investigated as illustrated in Figure 3, for potential solutions for this specific site and also future applications with different site conditions. These options are (a) direct water condensation, (b) indirect condensation with water in a closed loop and ambient air as heat sink, and (c) spray cooled air condensation. The rest of the system is kept the same as in Figure 1.

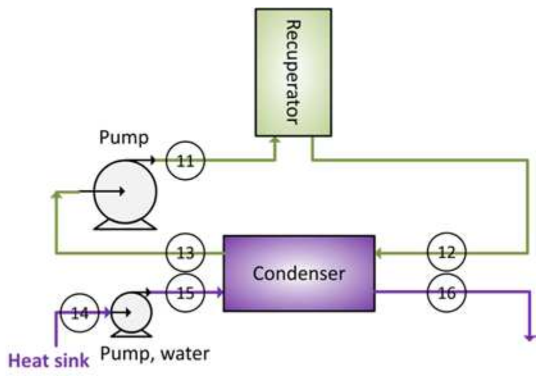

(a) Direct water condensation

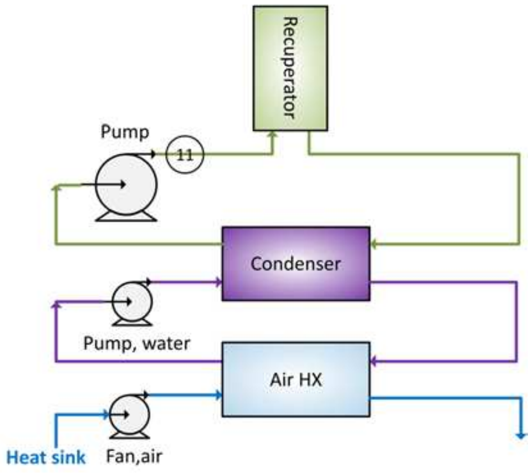

(b) Indirect condensation

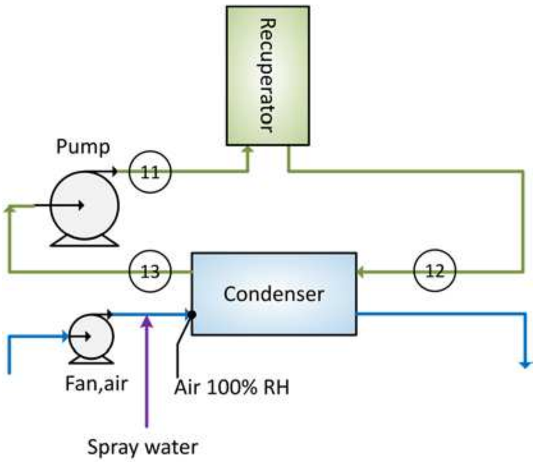

(c) Spray cooled air

Figure 3: Design options for air- and water-cooled condensation

With the direct water solution, the ambient air heat sink is replaced with water, using the same inlet temperature and a reduced temperature lift of 10 K. The temperature difference constraint is also lowered from 24 K to 10 K. The indirect condensation solution also uses water with the same specifications in the condenser, but in a closed air-cooled loop. The benefits of this would be a reduction in working fluid inventory and more freedom in choosing location of the heat sink. However, some performance reduction must be expected due to the additional heat exchange, and more space would be required for the additional heat exchanger and piping. The inlet temperature of the water was increased from 12.5 °C to 32.7 °C, based on an assumption that the water/air heat exchanger is similar in performance to the air-cooled condenser in the base case. This increases the condensation pressure of the cycle. The additional pump and fan work required for this is estimated using isentropic and isochoric efficiencies equal to the pumps and fans in the base case.

Using a spray tower to cool the air used in a direct air condenser would allow for a combination of more compact condenser and reduced condensation pressure. This configuration would require more space and water, both of which are restricted at the demonstration site. For this simulation, it is assumed that temperature of the spray-cooled air is equivalent to dry air cooled to its wet bulb temperature. A relative humidity value of 50 % has been considered, giving air at 12.5 °C a wet bulb temperature of 7.25 °C. Thus, compared to the base case, only the inlet air temperature was changed for the simulation. Any power required for additional auxiliaries with this solution is not included in this consideration.

3 RESULTS AND DISCUSSIONS

3.1 Cycle optimization results

With the boundary conditions described in section 2.1 and the parameter specifications in Table 1, a cycle with the layout as illustrated in Figure 1 achieves an optimized net power output of 1986 kW. The gross power output from the generator is 2252 kW, with the power consumption of the pumps and fans summing to 266 kW, of which the majority is needed for the heat sink fan and working fluid pump. All constraints listed in Table 1 are met. In addition, the variables *flue gas outlet temperature* and *heat sink temperature increase* are at their minimum allowed value and maximum allowed value respectively. Further details on the optimal solution for the base layout are shown in comparison with alternative layouts in Table 2 and Table 3.

3.2 Alternative cycle layouts

The comparison of the different configurations is summarized in Table 2. The thermal efficiency is calculated using the heat recovered from the off-gas as basis, while the exergy efficiency uses the exergy in this heat as well as the electrical input to the cycle.

Table 2: Comparison of system performances of the different configurations

		Base case: Recuperative, Indirect evaporation	**Non-recuperative, Indirect evaporation**	**Recuperative, Direct evaporation**
Net power	[kW_{el}]	1986	1657	2080
WHR HX duty	[kW]	9242	9242	-
Evaporator duty	[kW]	9248	9247	9242
Recuperator duty	[kW]	1928	-	2383
Condenser duty	[kW]	7047	7385	6954
WHR HX UA-value	[kW/K]	113	88	-
Evaporator UA-value	[kW/K]	564	404	106
Condenser UA-value	[kW/K]	370	303	365
Recuperator UA-value	[kW/K]	68	-	79
Thermal efficiency	[%]	21.5	17.9	22.5
Exergy efficiency	[%]	40.9	34.3	42.9

580

It can be seen that using a recuperator is highly beneficial in terms of power output, but at the cost of increased UA values for the other heat exchangers. This is due to a reduction in temperature difference in these heat exchangers, and indicates that a recuperative cycle will require more space and more costly components. Conversely, using an indirect cycle to recover the heat instead of direct evaporation has only a small cost in terms of power output at this nominal operation point, due to the working fluid reaching its maximum temperature in both cases. This loss would be further reduced if the increased uptime afforded by a thermal energy storage, which the indirect cycle enables, could be accounted for.

3.3 Alternative condensation options

The three alternative condensation options are compared with the direct air condensation in Table 3. For the direct water solution, water consumption is equal to water flowrate and is reported as such. Some make-up water would be required to cover leaks in the indirect solution, but this is not accounted for. For the spray cooling, it is assumed that liquid water can be recycled, so that only water that evaporates in the cooling tower is consumed. UA-values are also included as they can be used to indicate component size. However, they are not suited for direct comparison when using different fluids.

Table 3: Key results for various condenser options

		Base case: Direct with air	Direct with water	Indirect	Spray-cooled
Net power	[kW]	1986	2211	1838	2050
Condenser UA	[kW/K]	370	580	551	360
Water consumption	[kg/s]	-	165	-	1.083
Condensation pressure	[bar]	0.66	0.44	0.998	0.544
Condensation temperature	[°C]	36.7	25.9	48.7	31.4

3.4 Exergy analysis

In Figure 4 below, an overview of the exergy losses in the various cycle layouts are shown. In this figure, each column sums to the total exergy input to its respective cycle. This includes both the thermal exergy extracted from the off-gas, which is equal in all cases, and the electrical power supplied to the pumps and fans, which varies. The destruction of exergy in each component, either from temperature/pressure loss or from inefficiencies in conversion to/from electric power, is then subtracted from the total. Removing the exergy leaving the cycle in the heat sink leaves only the gross power output of the generator, which then finally gives the net power by subtracting the total power consumption. Exergy leaving the cycle unused in the off-gas, which is equal in all cases, is not included for readability.

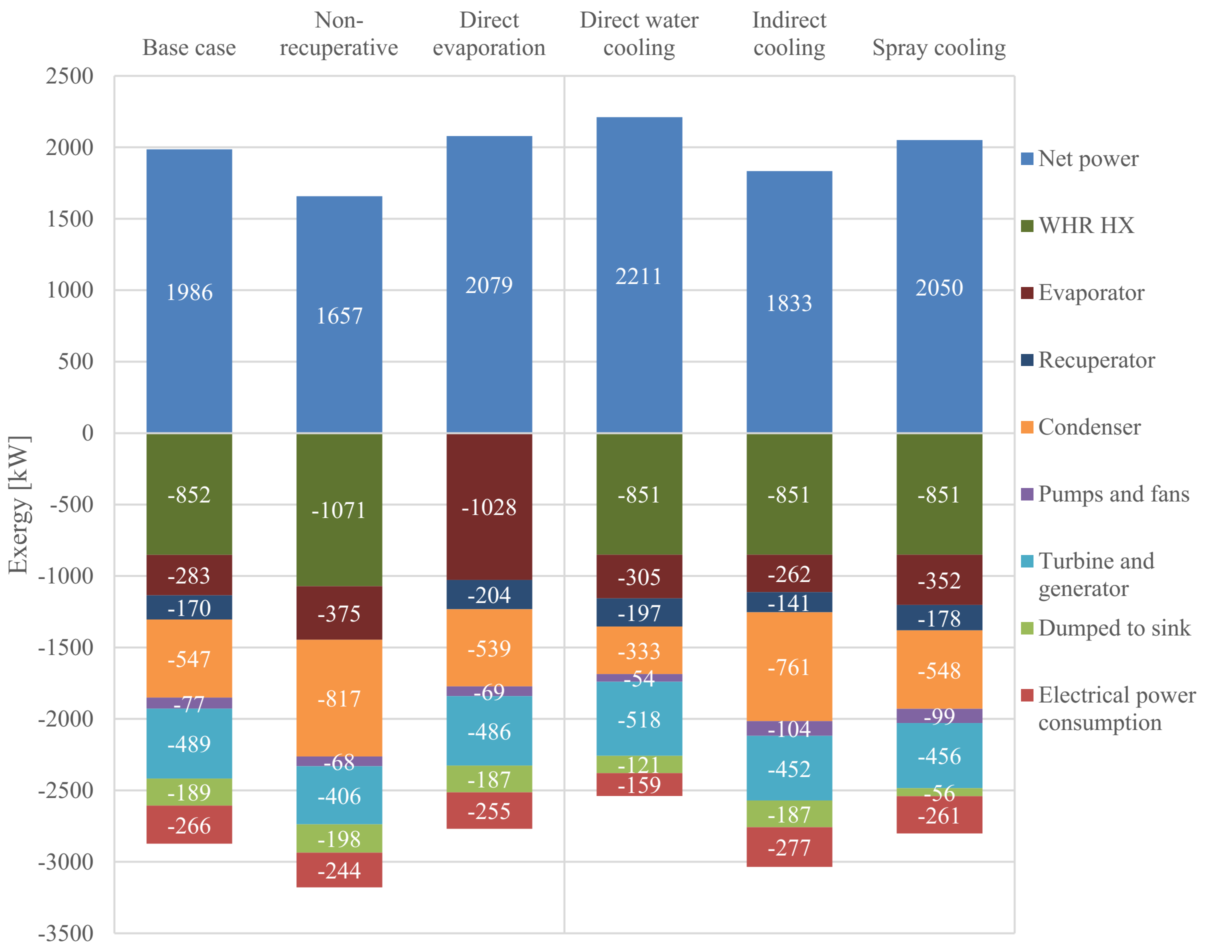

Figure 4: Comparison of exergy losses and resulting power output when optimizing the cycle with various design options, with cycle layouts on the left and condenser options on the right.

To the right in Figure 4, the losses in the entire cycle using the various condenser options are shown. In sites with water available for direct cooling a potential net power increase of 11 % is indicated, compared to the base case using an air-cooled condenser. The amount of exergy dumped to the sink is significantly lowered with the spray-cooled solution, and could be investigated for sites with more space available. Lastly, if an indirect cooling loop has to be used, a net power loss of 8 % can be expected, mainly from the additional temperature loss driving the condensation system.

SUMMARY

In this work, a comparison of designs with optimized operating conditions of an ORC for a future demonstration pilot in an iron & steel plant located in Czech Republic is presented. A system optimization model is developed to maximize the net power output, while satisfying practical limitations, for a heat source design point determined from historical site data. A configuration using indirect heat recovery with an oil loop, recuperative working fluid cycle, and direct air condensation, is used for the base design as it is considered the most suitable to cope with variations of the heat source conditions and the availability of the heat sink. This configuration is optimized against the practical constraints and provides a net power output of 1986 kW with 21.5% and 40.9% in the thermal and exergy efficiency, respectively.

To investigate other potential solutions for this site and expand the applicability of the design for future ORC implementation, alternative designs are also evaluated and compared with the base configuration. The non-recuperative working fluid cycle significantly reduces the net power output by 16%, but may require less space. The direct heat recovery design has a similar level of power output thus is less attractive for the scenario with large variation in heat source. Additionally, several condenser options (direct air; indirect and direct with water; spray-cooled air) are assessed and compared. The direct condensation with water gives the largest power output while the indirect water condensation with a closed air-cooled loop gives the smallest. For the current site conditions, direct air condensation is the most reasonable solution, while the other options have their own advantages and should be considered based on the practical requirements. Exergy analyses for the alternative designs are performed to illustrate the performance losses in the various components and to give insights for future improvement of the design. The results and analyses of the system design will serve as the basis for performance specification and detailed design of all main system components towards finalizing the design of the demonstrator. Also, it provides references to future waste heat recovery applications and ORC implementations. 582

REFERENCES

Bianchi, G., Panayiotou, G.P., Aresti, L., Kalogirou S.A., Florides G.A., Tsamos K., Tassou S.A., Christodoulides P., 2019, Estimating the waste heat recovery in the European Union Industry. *Energ. Ecol. Environ.* vol. 4: p. 211-221.

Bell, I., 2013, NIST Reference Fluid Thermodynamic and Transport Properties Database (REFPROP) Version 9 - SRD 23, *National Institute of Standards and Technology*.

Bell, I., Wronski, J., Quoilin, S., Lemort, V., 2014, Pure and Pseudo-pure Fluid Thermophysical Property Evaluation and the Open-Source Thermophysical Property Library CoolProp. *Ind. Eng. Chem. Res*. vol. 53, no. 6: p. 2498-2508.

Braimakis, K., Preißinger, M., Brüggemann, D., Karellas, S., Panopoulos, K., 2015, Low grade waste heat recovery with subcritical and supercritical Organic Rankine Cycle based on natural refrigerants and their binary mixtures, *Energy*, vol. 88: p. 80-92.

Deng, H., Hagen, B., Nikolaisen, M., Andresen, T., 2020, Comparing three methods for design analyses of rankine cycle for waste heat recovery from natural gas compression. *Refrigeration Science and Technology*. vol. 2020-July: p. 249-256.

Deng H., Andresen T., Skaugen G., Gladysz P., Pajak L., Sowizdzal A., Miecznik M., 2022. Topside cycles for enhanced geothermal systems with CO_2 and hydrocarbons as working fluids. *15th IIR-Gustav Lorentzen Conference on Natural Refrigerants*. Trondheim, Norway, June 13-15th 2022.

EPA, 2013, Transitioning to Low-GWP Alternatives in Building and Construction Foams. EPA, Washington, D.C.
Hagen, B.A.L., Nikolaisen, M., Andresen, T., 2020. A novel methodology for Rankine cycle analysis with generic heat exchanger models. *Appl. Therm. Eng.* vol. 165: 114566.
IEA, 2021, Net Zero by 2050. IEA, Paris.
Lai, N.A., Wendland, M., Fischer, J., 2011, Working fluids for high-temperature organic Rankine cycles, *Energy*, vol 36, no. 1: p. 199-211.
Lecompte, S., van den Broek, M., & De Paepe, M., 2015, Performance potential of ORC architectures for waste heat recovery taking into account design and environmental constraints, *3rd International Seminar on ORC Power Systems*. Brussels, Belgium October 12-14th 2015.
Schittkowski, K., 1986, NLPQL: A fortran subroutine solving constrained nonlinear programming problems. *Ann. Oper. Res*. vol. 5: p. 485-500.

ACKNOWLEDGEMENT

This work has been part of the DECAGONE project, funded by the European Union's Horizon Europe research and innovation programme under grant agreement No 101069740.

This book contains the compilation of works contributed to the *7th International Seminar on Organic Rankine Cycle Power Systems* (ORC 2023), held in Seville between the 4th and 6th of September 2023. The event was hosted by Universidad de Sevilla on behalf of the Knowledge Centre on Organic Rankine Cycle Technology (KCORC), incorporated in The Netherlands.

The ORC conference, organized biennially, stems as the only conference that is specific to ORC technology, therefore gathering a diverse community whose affiliation spans across all the interested stakeholders, not only in this particular technology but also and in a broader context, in the energy transition. Original equipment manufacturers, professional associations, end-users, investors, policy makers, academics, scientists feel at home at ORC 2023.

The almost 100 proceedings in this book cover a wide variety of topics, from fundamentals to system integration through component design, accounting for thermodynamic performance as well as component design. In addition to this, and as a new track in 2023, works on heat pump technology were also accepted in order to raise awareness of the strong ties between both technologies, specifically in energy storage applications.

This book provides an excellent overview of the current maturity of power systems based on Organic Rankine Cycle technology for applications as diverse as geothermal and waste heat recovery in industry or downstream of other prime movers (e.g., marine applications). It is also an excellent source of information to understand the current challenges faced by the technology, stemming from a very competitive market and increasingly stringent environmental regulations.

The organizers of ORC 2023 hope that the reader finds this work as exciting as the attendees to the conference and, maybe, make the decision to join the 8th edition to the conference in 2025.

KCORC
KNOWLEDGE CENTER
ORGANIC RANKINE CYCLE

eus EDITORIAL
UNIVERSIDAD DE SEVILLA